Identifying and Characterizing Binding Sites on the Irreversible Inhibition of Human Glutathione S-Transferase P1-1 by *S*-Thiocarbamoylation

Indalecio Quesada-Soriano, Alessandra Primavera, Juan M. Casas-Solvas, Ramiro Téllez-Sanz, Carmen Barón, Antonio Vargas-Berenguel, Mario Lo Bello, Luís García-Fuentes

Graphical Abstract

Irreversible modification: We report the inactivation of GST P1-1 with *S*-(*N*-benzylthiocarbamoyl)glutathione through the covalent modification of two Cys47 residues per dimer and one Cys101. This covalent inhibition is revealed at physiological temperatures, at which the BITC moiety is covalently bound to these enzyme cysteines through an S-thiocarbamoylation reaction.

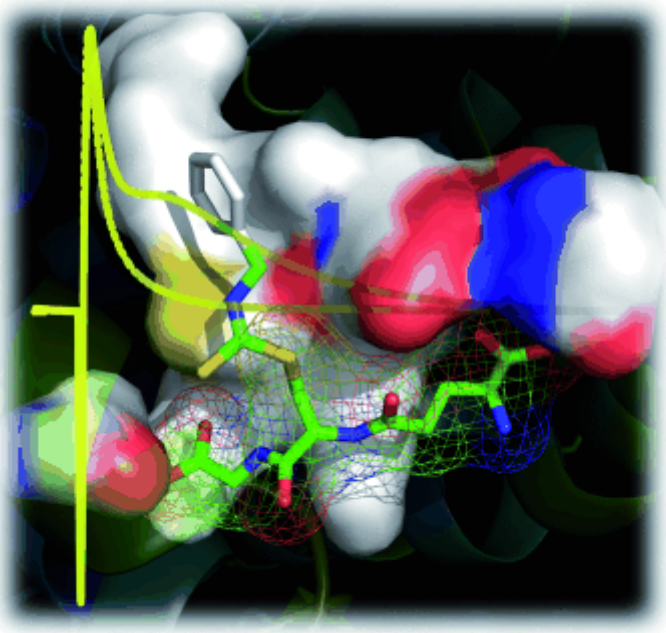

Abstract

Human glutathione S-transferase P1-1 (hGST P1-1) is involved in cell detoxification processes through the conjugation of its natural substrate, reduced glutathione (GSH), with xenobiotics. GSTs are known to be overexpressed in tumors, and naturally occurring isothiocyanates, such as benzyl isothiocyanate (BITC), are effective cancer chemopreventive compounds. To identify and characterize the potential inhibitory mechanisms of GST P1-1 induced by isothiocyanate conjugates, we studied the binding of GST P1-1 and some cysteine mutants to the BITC–SG

conjugate as well as to the synthetic *S*-(*N*-benzylcarbamoylmethyl)glutathione conjugate (BC–SG). We report here the inactivation of GST P1-1 through the covalent modification of two Cys47 residues per dimer and one Cys101. The evidence has been compiled by isothermal titration calorimetry (ITC) and electrospray ionization mass spectrometry (ESI-MS). ITC experiments suggest that the BITC–SG conjugate generates adducts with Cys47 and Cys101 at physiological temperatures through a corresponding kinetic process, in which the BITC moiety is covalently bound to these enzyme cysteines through an S-thiocarbamoylation reaction. ESI-MS analysis of the BITC–SG incubated enzymes indicates that although the Cys47 in each subunit is covalently attached to the BITC ligand moiety, only one of the Cys101 residues in the dimer is so attached. A plausible mechanism is given for the emergence of inactivation through the kinetic processes with both cysteines. Likewise, our molecular docking simulations suggest that steric hindrance is the reason why only one Cys101 per dimer is covalently modified by BITC–SG. No covalent inactivation of GST P1-1 with the BC–SG inhibitor has been observed. The affinities and inhibitory potencies for both conjugates are high and very similar, but slightly lower for BC–SG. Thus, we conclude that the presence of the sulfur atom from the isothiocyanate moiety in BITC–SG is crucial for its irreversible inhibition of GST P1-1.

Introduction

A number of studies support the fact that certain food phytochemicals are effective chemoprotective agents against chemical carcinogenesis. An important group of compounds that have this property are organosulfur compounds such as isothiocyanates (i.e., sulforaphane and benzyl and allyl isothiocyanate).1 Isothiocyanates inhibit rat lung, esophagus, mammary gland, liver, small intestine, colon, and bladder tumorigenesis.2, 3 These compounds are derived from the hydrolysis of glucosinolates that occur in a variety of cruciferous vegetables such as cabbage, cauliflower, and broccoli and are widely consumed by humans; that is, isothiocyanates might be part of the active ingredients of these foods.1a,1e All isothiocyanates are characterized by the presence of a -N=C=S group, and certain studies indicate that their biological activity can be mediated through reaction of the electrophilic central carbon of -N=C=S with cellular nucleophilic targets.1b

Some authors have shown that organic isothiocyanates undergo conjugation with glutathione (GSH) either enzymatically (by GST-driven catalysis) or nonenzymatically to dithiocarbamates.3, 4 The enzyme families of GSTs (EC 2.5.1.18) catalyze the conjugation of the tripeptide glutathione (GSH; γ-Glu-Cys-Gly) to electrophilic centers of a wide variety of potentially harmful compounds. This reaction generates other soluble conjugates in water that

can be further metabolized and eventually excreted. The common feature of the enzymatic conjugation reaction is the attachment of the thiol group of GSH to an organic electrophile such as an isothiocyanate. Moreover, these compounds might also react with nucleophilic amino acid residues of cellular proteins. The potential binding sites include thiol-containing cysteine and amine-containing amino acids such as lysine and arginine.3 Among these sites, cysteines residues are the most nucleophilic in proteins and are therefore the most likely binding sites.3, 5 Moreover, recently some authors have demonstrated that S-thiocarbamates can modify cysteine residues in some proteins by a transthiocarbamoylation reaction.6

In mammals, there are two major families of soluble GSTs, located in the cytosol and mitochondria. These are dimeric enzymes, composed of two-domain subunits which can be grouped into at least eight gene-independent classes on the basis of their primary structure.7 Most of the GSH-binding amino acid residues forming the G site are located in the N-terminal domain with a thioredoxin fold, whereas the C-terminal region makes the most contacts with the electrophilic substrate and defines the H site. The diverse functions, including catalytic GSH conjugation, passive ligandin-type binding, and modulation of signal transduction, may be selectively targeted by different inhibitors.

Among the various GSTs, the Pi class (GST P1-1) has attracted attention because it is overexpressed in a variety of malignancies, including lung, colon, ovary, esophageal, and stomach cancers.8 Furthermore, a number of studies have shown a correlation between overexpression of GST P1-1 and the development of resistance toward various anticancer drugs. Thus, human GST P1-1 inhibitors are emerging as promising therapeutic agents for managing the development of resistance among anticancer agents.9 Therefore, the use of selective inhibitors to modulate GST P1-1 activity during chemotherapy is a promising strategy in the battle against multidrug resistance that could result in enhanced therapeutic efficiency of anticancer compounds. Many compounds have been described in the literature as GST inhibitors, including GSH analogues, GSH conjugates, small organic molecules, and natural products.9c, 10 Perhaps the most explored strategy for the development of GST inhibitors has been the conjugation of GSH, through its thiol group, to a variety of structural moieties. The rationale for this strategy is based on the observation that GSTs are subject to product inhibition.11 Inhibition of GST P1-1 can be reversible or irreversible and an extensive list of reversible inhibitors are presented in literature.10b Irreversible inhibitors modify the enzyme by covalent binding, resulting in a permanent loss of activity.12 Thus, a promising approach for improving the specificity of enzyme inactivation resides in enzyme-activated irreversible

inhibitors (mechanism-based inhibitors). Mechanism-based inhibitors exhibit great potency due to their high binding affinity for the target enzyme generating reactive electrophiles which inactivate the enzyme by covalent attachment.13 GST P1-1 class cysteine residues are known to be susceptible to covalent modification by electrophiles, with the two most reactive and solvent accessible of these residues located at positions 47 and 101.14 In particular, Cys47, which is located close to the active site, has been observed to be reactive and accessible for electrophilic compounds.15 Covalent modification of this cysteine residue results in loss of enzyme activity.16 In addition, Cys101 is located at the dimer interface but can form a disulfide bridge with Cys47, requiring a large-scale conformational change of the active site leading to inactivation of the enzyme. Identification of molecular targets by isothiocyanates can provide useful information on the enzyme mechanism and future drug design. Some authors have shown that Cys47 and Tyr 103 are the targets of benzyl isothiocyanate (BITC).17 BITC, similarly to ethacrynic acid (EA), is a substrate of GSTs, with the Pi class being the most efficient catalyst.4a In this study, we examined the interaction of the *S*-(*N*-benzylthiocarbamoyl)glutathione (BITC–SG) conjugate with GST P1-1 by titration calorimetry, fluorescence spectroscopy, and docking studies. This conjugate irreversibly inhibits the enzyme through formation of covalent adducts, which are evident at physiological temperatures. Thus, the goals of the present study were to identify the binding sites of BITC–SG and the targets responsible for the formation of covalent adducts, following the assumption that the reactive Cys47 and Cys101 side chains were determinants for specific inactivation of GST by dithiocarbamates. Electrospray ionization (ESI) mass spectrometry has been used to identify these direct covalent interactions. The C47S/C101S double mutation removes any covalent modification of the enzyme by BITC–SG. Alternatively, we synthesised another GSH conjugate, *S*-(*N*-benzylcarbamoylmethyl)glutathione (BC–SG), an analogue of BITC–SG that contains a carbamoyl □NH□CO□ group instead of the dithiocarbamoyl □NH□CS□S□ group. This synthetic conjugate showed very similar binding behavior but without any covalent modification of the enzyme.

Identifying and characterizing the isothiocyanate and derivative binding sites on target proteins is critical to decipher the mechanisms of isothiocyanate-induced cellular effects. Not only do these studies provide mechanistic insights, but they also shed light on a molecular basis for drug optimization and screening.

Results

Binding to wild-type (wt) enzyme

Isothermal titration calorimetry (ITC) has been used to investigate the interaction of the BITC–SG conjugate with wt-GST P1-1 across a temperature range from 8–42 °C. Figure 1 A shows a regular ITC profile for the binding of BITC–SG to dimeric wt-GST P1-1 in phosphate buffer at pH 7.0 and 11.0 °C. The binding is exothermic at all temperatures studied with high affinity. The order of K_d values (K_d~1.6 µM) reflects the inhibitor potency of this conjugate compared to their parent compounds (K_d(GSH)~86 µM,18 K_d(BITC)~650 µM17). Fluorescence titrations of the enzyme with BITC–SG gave quenching curves consistent with the calorimetric behavior (Table 1).

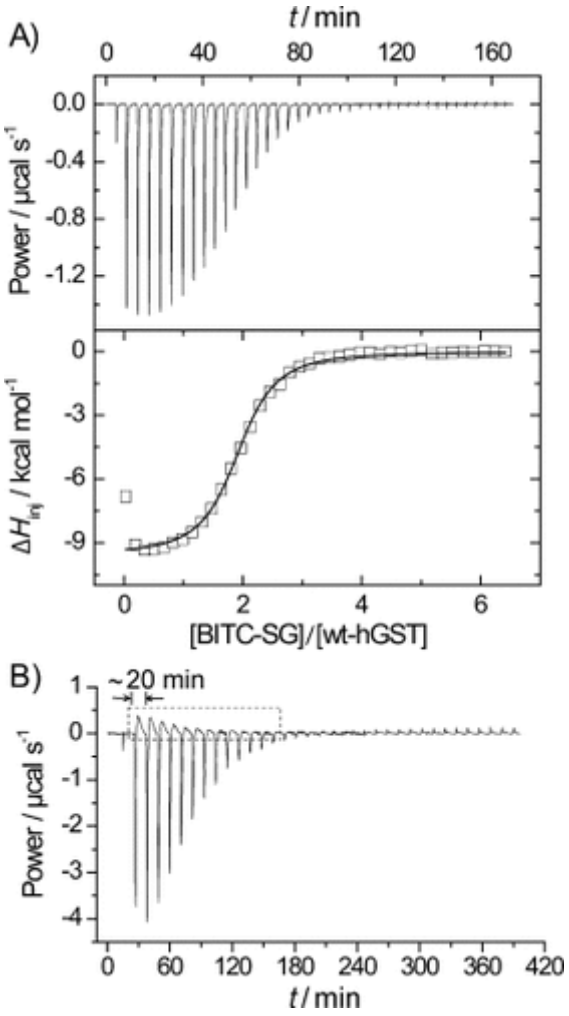

Figure 1 Representative isothermal titration calorimetry (ITC) measurements of the binding of BITC–SG to wild-type GST P1-1. A) The calorimetric titration corresponds to 20.07 µM of dimeric GST P1-1 with 39-5 µL injections of 0.9 mM BITC–SG at 11 °C. A preinjection of 1 µL was performed at the start of the experiment. B) Exemplary calorimetric thermogram for the titration of 25.66 µM of dimeric wt-GST P1-1 with 34-5 µL injections of 3 mM BITC–SG at 39.1 °C. A preinjection of 1 µL was also performed at the start of the experiment. Titrations were performed in 20 mM sodium phosphate, 5 mM NaCl, and 0.1 mM EDTA at pH 7.0.

Table 1. Thermodynamic parameters for BITC–SG and BC–SG binding to wt-GST P1-1 in phosphate buffer as a function of temperature at pH 7.0.

Inhibitor		Fluorescence	Calorimetry			
	T [°C]	$K\times10^{-5}$ [M^{-1}]	$K\times10^{-5}$ [M^{-1}]	$-\Delta G^0$ [kcal mol^{-1}]	$-\Delta H$ [kcal mol^{-1}]	$-T\Delta S^0$ [kcal mol^{-1}]
BITC–SG	8.2	7.2±1.6	10.3±0.7	7.71±0.4	9.4±0.1	1.65±0.2
	11.0	6.4±0.8	8.9±0.5	7.70±0.2	9.6±0.1	1.93±0.3
	15.1	6.9±1.4	8.2±0.4	7.77±0.2	10.1±0.2	2.28±0.2
	19.3	5.3±2.5	6.3±0.2	7.73±0.1	10.6±0.2	2.91±0.2
	23.2	4.2±1.8	3.3±0.4	7.45±0.2	11.0±0.1	3.54±0.1
BC–SG	19.2	3.5±1.4	5.73±0.3	7.67±0.2	12.5±0.3	4.83±0.2
	25.2	3.1±2.0	3.46±0.2	7.54±0.2	13.7±0.3	6.18±0.1
	31.0	2.2±0.8	1.71±0.1	7.26±0.1	15.1±0.2	7.76±0.2
	42.0	2.7±0.4	1.94±0.1	7.60±0.2	16.7±0.2	9.08±0.3

Nevertheless, it is crucial to observe the calorimetric traces obtained at temperatures above 25 °C (for instance at 39.1 °C; Figure 1 B). A detailed examination of these calorimetric thermograms revealed important features. The calorimetric response after each injection of BITC–SG (thermogram peaks) shows two well-time-differentiated phases: a faster exothermic phase along with a slower endothermic phase. This slower endothermic contribution increases and becomes more defined with an increase in temperature, but decreases when the [BITC–SG]/[enzyme] ratio in the calorimetric cell increases. At 25 °C, this endothermic and slower phase is not yet observed, though the measured enthalpy change has a smaller absolute value than that theoretically deduced by the ΔC_p calculated from temperatures <25 °C, assuming ΔC_p is constant across the temperature range. The slow endothermic contribution becomes visible as a distinct calorimetric phase at 31 °C. The calorimeter response time for the exothermic phase is shorter than that for the endothermic phase and comparable to the response times for dilution experiments or typical binding processes. This fact is easily

understood when comparing the thermograms in Figure 1 A and B. Therefore, the presence of these two distinct time phases reveals the occurrence of at least two separable steps upon ligand–protein complex formation. The first and fast process is the binding of BITC–SG to the protein and the second corresponds to a slow process concomitant to the binding process.

ITC thermograms at temperatures below 25 °C show no trace of this slow endothermic contribution. To find out if this was simply due to this second phase occurring much more slowly at these temperatures, we incubated the protein under the same ITC conditions with BITC–SG for 3 h and performed an EMS analysis afterward. EMS results showed the absence of any chemical modification of the enzymes. Analysis of the thermograms at temperatures below 25 °C provides a good fit to a model of two equal and independent sites of GST dimerization. The binding, as expected for a GSH-conjugate, should be to the G and H sites in each GST P1-1 subunit. This was corroborated by ITC experiments in which an EASG inhibitor saturated enzyme (K_d~0.5 μM, a greater affinity than that for BITC–SG)19 was titrated with BITC–SG at 20 °C. The thermograms obtained show no binding of BITC–SG to wild-type enzyme. This indicates that the binding of both conjugates is competitive with a higher association constant for EASG. Moreover, a slow process is not observed at 20 °C.

The binding constants and enthalpy changes for the binding of BITC–SG to GST P1-1 between 8 and 23 °C are displayed in Table 1. The enthalpy change varies linearly with temperature (Figure 2 A) and provides a ΔC_p^0 value of −115±12 cal mol^{-1} K^{-1}.

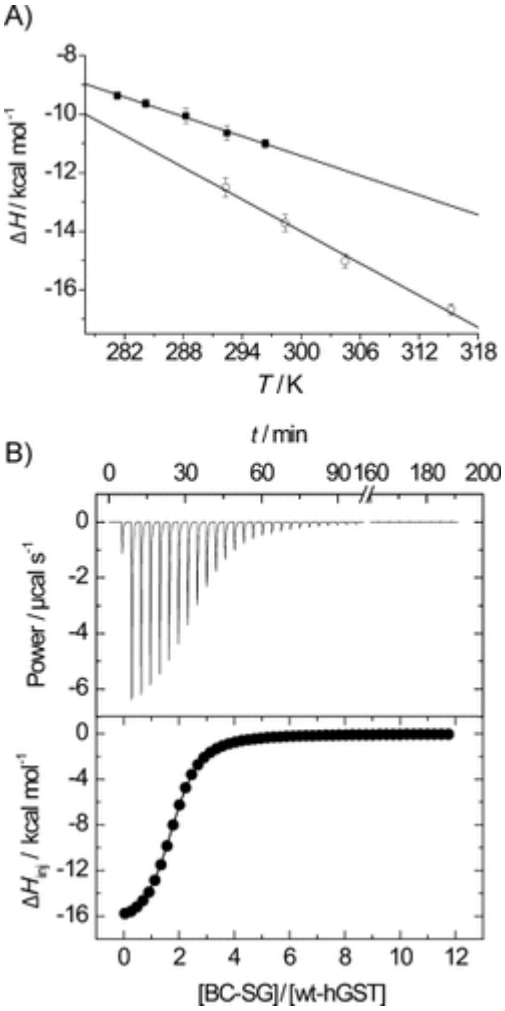

Figure 2 A) Temperature dependence of the enthalpy change for the binding of BITC–SG (▪) and BC–SG (○) to dimeric wt-GST P1-1. The heat capacity changes, associated with the binding, were determined from the slopes of linear regression analysis. B) Representative ITC measurements of the non-cooperative binding of 2.5 mM BC–SG to 25.6 µM dimeric wild-type GST P1-1. Titration was performed in 20 mM sodium phosphate, 5 mM NaCl, and 0.1 mM EDTA at pH 7.0 and 42 °C.

However, the ITC thermograms obtained at temperatures ≥25 °C cannot be fitted to any typical binding model because the slow process concomitant to regular binding would provide incorrect thermodynamic parameters. This slow process might be due to the covalent modification of an enzyme residue triggered by the previous binding of BITC–SG. The highly reactive Cys47, which is close to the G and H sites, appears to be a good candidate target of such covalent modification. Under this hypothesis, the BITC–SG interaction with the enzyme can be schematized in two steps. In step 1, the protein binds exothermically and reversibly in a non-cooperative manner to BITC–SG, occluding the G and H sites in each subunit. This step is common at every temperature and represents typical noncovalent binding. In step 2, the initial

complex rearranges in such a way that Cys47 covalently reacts with the thiocarbonyl carbon of the BITC–SG conjugate (see Scheme 1). This kinetic step will be temperature-dependent according to the Arrhenius' equation.

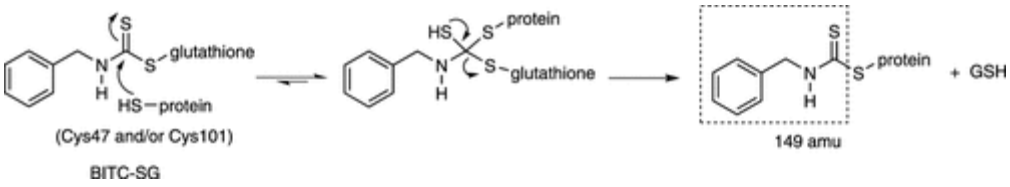

Scheme 1

If the slow process is due to such a reaction, it should not occur during the binding of BC–SG to wt-GST because in this case, the BC–SG amide carbonyl carbon is not as good of an electrophile as the dithiocarbamoyl C□S carbon. To test this statement, ITC experiments with BC–SG and GST P1-1 were conducted at various temperatures between 19 and 42 °C under the same solution conditions as those described for the BITC–SG conjugate. In this case, the BC–SG interaction with the wild-type enzyme generates calorimetric thermograms typical of exothermic and non-cooperative intrinsic binding, with no slow phases appearing at any temperature (e.g., 42 °C, Figure 2 B). Equally, fluorescence titrations of the wild-type enzyme with BC–SG resulted in curves with association constants similar to those determined by calorimetry (Table 1).

The binding stoichiometry, deduced from the calorimetric curves, was two conjugate molecules per enzyme dimer. Also, the absence of BC–SG binding to an EASG-saturated enzyme indicated the competition between these ligands for the G and H sites of the enzyme and the lower affinity of the BC–SG conjugate as compared to EASG. A model of two equal and independent sites fits well to the experimental data at the temperatures studied. The enthalpy change values vary linearly with temperature according to a ΔC_p^0=−185±33 cal mol^{-1} K^{-1} (Figure 2 A). The values for ΔG^0, ΔH and ΔS^0 are given in Table 1.

Inhibition studies of wild-type GST P1-1 with BITC–SG and BC–SG

Upon incubation of GST P1-1 with different amounts of BITC–SG and BC–SG, we observed an inhibitory effect of these compounds. The IC_{50} values, reported in Table 2, were 92.85 μM for BITC–SG and 115.90 μM for BC–SG. These values showed similar inhibitory potency for these two inhibitors. Moreover, these compounds showed a competitive inhibitory behavior towards GSH. K_i(GSH) values of 10.87 and 22.20 μM were obtained for BITC–SG and BC–SG, respectively (Table 2), from double-reciprocal plots.

Table 2. IC_{50} values and inhibition constants (K_i) for BITC–SG and BC–SG binding to GST P1-1 at 25 °C

Compound	IC_{50} [μM]	K_i(GSH) [μM]
BITC–SG	92.85±0.05	10.87±0.02
BC–SG	115.90±0.09	22.20±0.01

Binding to cysteine mutants

In order to identify the potential targets responsible for the kinetic processes observed upon binding of BITC–SG to GST P1-1, we also studied the interaction of this conjugate with various cysteine mutants (C47S, C101S, and C47S/C101S) of the protein. For the wild-type enzyme, the kinetic processes are clearly detected and observed at temperatures close to the physiological range but are not detected at temperatures below 25 °C, therefore we examined the binding of this conjugate to the mutants by ITC, particularly at temperatures higher than 25 °C. For instance, Figure 3 A shows a calorimetric thermogram obtained for its binding to C47S mutant at 42 °C. It is clear that the interaction of BITC–SG with this mutant still shows a kinetic process associated with the binding. Therefore, the C47S mutation does not remove the slow phase detected in the wild-type enzyme. However, the thermogram is, in this case, sigmoidal and characteristic of a process with positive cooperativity, which is expected for the binding of ligands to the G site in the Cys47 mutants.19–23

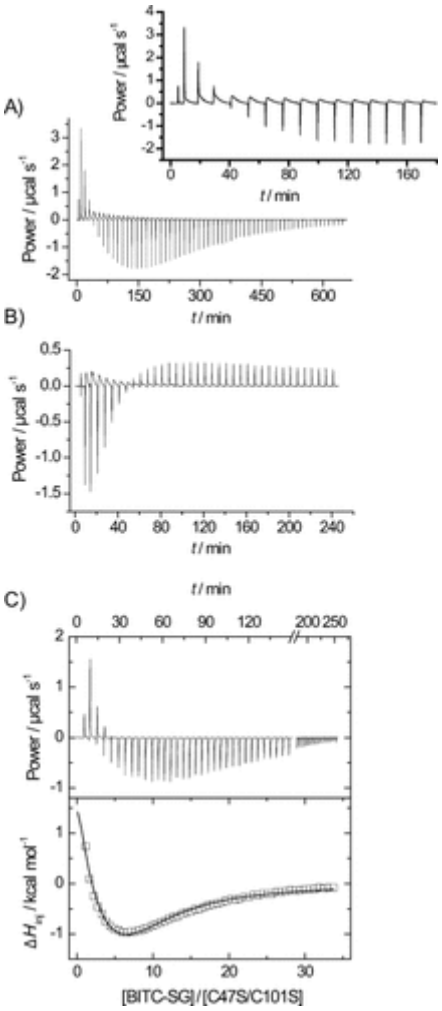

Figure 3 Representative calorimetric thermograms for the BITC–SG interaction with cysteine mutants of GST P1-1. A) Titration of 25 µM dimeric C47S mutant with 5 µL injections (1 µL first injection) of 4.5 mM BITC–SG at 42 °C. The first peaks are shown as an inset plot for better visualization of the kinetic process. B) Titration of 20 µM of the dimeric C101S mutant with 5 µL injections (1 µL first injection) of 3 mM BITC–SG at 38 °C. C) Calorimetric measurements of the cooperative binding of 4.5 mM BITC–SG (5 µL injections) to 30 µM of the dimeric C47S/C101S double mutant at 39 °C. The bottom panel shows the fit to a cooperative model with K_1=2.1×10^3 M^{-1}, K_2=1.4×10^4 M^{-1}, ΔH_1=24.5 kcal mol^{-1} and ΔH_2=−42.3 kcal mol^{-1}. Titrations were performed in 20 mM sodium phosphate, 5 mM NaCl, and 0.1 mM EDTA at pH 7.0.

Analogous ITC experiments to those described for the C47S mutant were performed with the C101S mutant. Similarly, at high temperature (e.g., 38 °C), a kinetic process is clearly visible (Figure 3 B). In this case the binding is not cooperative, as the Cys47 residue, responsible for induced cooperativity by ligands, is intact. Like the wild-type enzyme, the slow phase is not detected at temperatures below 25 °C for these two mutants (C47S and C101S).

In contrast, the calorimetric thermograms for the C47S/C101S double mutant and the BITC–SG conjugate at high temperatures (e.g., 39 °C in Figure 3 C) do not show the presence of the slow kinetic processes emerging with the wild-type and the simple mutants C47S and C101S. Instead, the response time of the calorimetric peaks is typical of noncovalent binding. A similar result was described for the binding of EA to GST P1-1.[19, 23] The observed profile is sigmoidal and characteristic of binding with positive cooperativity. A model of two equal and interacting sites (Figure 3 C) is able to perfectly fit the calorimetric data obtained from this double mutant at each temperature.

The existence of two slow phases associated with the covalent modifications of Cys47 and Cys101 can be visualized in Figure 4. This figure corresponds to a single injection (20 μL) of a large excess of BITC–SG conjugate (∼12 mM) into the calorimetric cell containing a solution of either wild-type enzyme (35.5 μM) or the C101S mutant (33.5 μM) at 39 °C. In both cases, the calorimetric traces show an initially fast and globally exothermic phase corresponding to previous processes (ligand dilution and binding) and an endothermic second phase corresponding to the kinetic processes. When comparing the two peaks in Figure 4, it is obvious that the trace for the wild-type enzyme shows two overlapping and endothermic slow phases, one faster than the other, whilst in the case of the C101S trace, only the faster one appears. This fact, along with the lack of slow phases in the case of the C47S/C101S double mutant, allows us to postulate that the two slow phases observed in the trace of the wild-type enzyme in Figure 4 correspond to the covalent modification of Cys47 (the faster slow phase) and Cys101 (the slower slow phase).

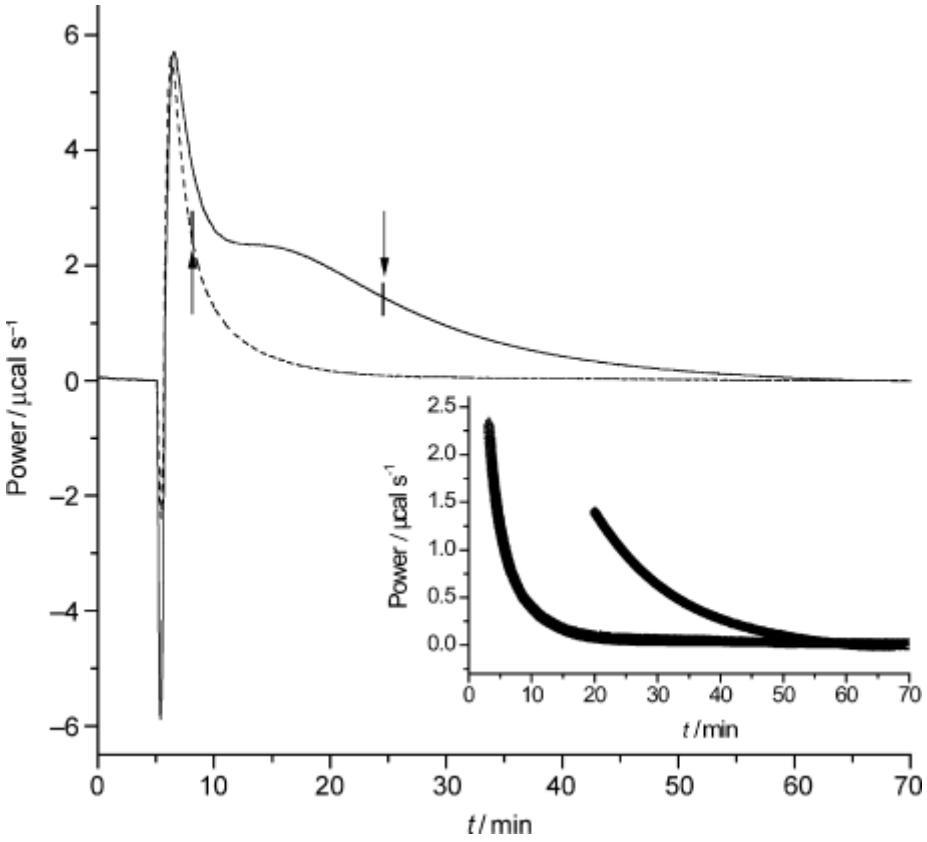

Figure 4 Calorimetric signals (heat flow versus time) corresponding to a single injection of 12.2 mM BITC–SG (20 µL) into the calorimetric cell (1.42 mL) containing 35.5 µM of dimeric wild-type (—) or 33.5 µM of C101S mutant (- - - -) of GST P1-1. These experiments were performed in 20 mM sodium phosphate, 5 mM NaCl, and 0.1 mM EDTA at pH 7.0 and 39 °C. Inset: Kinetic constants were deduced from analysis of time decay of the heat flow (arrow) assuming pseudo-first-order kinetics (see text for details).

The kinetic constants for both reactions were calculated by analyzing the time decay of the heat flow and assuming pseudo first order kinetics.19, 24 Analysis of the collected data indicates that it obeys monoexponential kinetics under the experimental conditions employed. Thus, two kinetic constants of 1.4×10^{-3} s^{-1} and 4.6×10^{-3} s^{-1} were determined for the reactions with Cys101 and Cys47, respectively.

On the other hand, binding of the BC–SG conjugate to the C47S, C101S, and C47S/C101S mutants under similar conditions to those described for BITC–SG generates calorimetric thermograms lacking any kinetic process and typical of noncovalent binding to two sites. Binding to the C47S and C47S/C101S mutants also show the expected positive cooperativity upon mutation of the Cys47.

Mass spectrometry and chemical modification with DTNB

Mass spectrometry is commonly used to identify post-translational modifications of proteins as well as direct covalent interactions between proteins and small molecules. To gain direct evidence of the S-thiocarbamoylation of hGST P1-1, we carried out ion spray ionization mass spectrometry (ESI) of the modified enzymes, both wt-GST P1-1 and the C47S and C47S/C101S mutants. The results are shown in Figure 5. Ion spray mass spectra of the unmodified wild-type GST P1-1 (Figure 5 A) showed two main peaks corresponding to molecular masses of 23 225 and 23 356 Da, respectively. The mass peak of 23 225 Da corresponds to that calculated from its cDNA sequence, whereas the mass peak of 23 356 Da is attributed to the failed removal of the N-terminal methionine residue.12a, 25

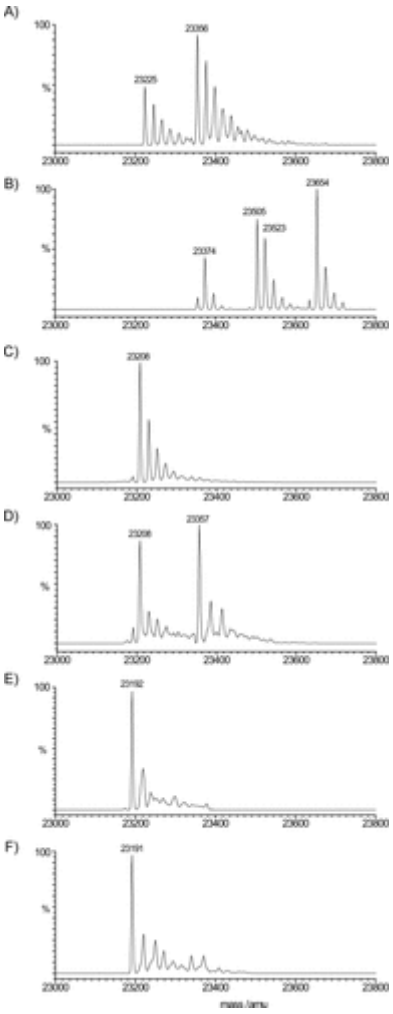

Figure 5 Deconvoluted electrospray ionization mass spectra of A) and B) wild-type hGST P1-1, C) and D) the C47S mutant, and E) and F) the C47S/C101S mutant. A), C), and E) ligand-free enzymes incubated at 37 °C for 3 h (control samples); B), D), and F) enzymes incubated with BITC–SG at 37 °C for 3 h (see the Experimental Section for details). Additional peaks of decreased intensity appear after the main peaks due to sodium addition (from buffer solution) during the ionization process in the positive ion detection mode.

Ion mass spectra for the BITC–SG-incubated enzyme as described in the Experimental Section were also recorded, and two series of peaks were obtained (Figure 5 B). The first series consists of two peaks of 23 374 and 23 505 Da, and the last series also shows two peaks but at 23 523 and 23 654 Da. These results, when compared to those obtained with the unmodified wild-type enzyme, indicate the formation of two covalent adducts with the subunits of the dimeric protein. Moreover, the peaks corresponding to the unmodified enzyme do not appear in the mass spectra of the BITC–SG-incubated enzyme. This indicates the absence of unmodified subunits after treating the wild-type enzyme with the BITC–SG conjugate for 3 h at 37 °C (see Experimental Section for details). In particular, the two peaks appearing in the first series correspond to the molecular mass calculated from the cDNA sequence, M^++149 (23 374 Da) or M^++298 (23 523 Da), respectively. Likewise, the second series corresponds to increments of +149±1 and +298±1 Da in the 23 356 Da peak of the unmodified enzyme.

The +149 Da increment in the molecular masses might correspond to one BITC moiety from the BITC–SG conjugate attached covalently to a protein subunit, presumably to Cys47 or Cys101, according to the reaction shown in Scheme 1, whilst the +298 Da increment would represent a subunit with both cysteines covalently modified. Therefore, these spectra demonstrate the simultaneous presence of mono- and di-thiocarbamoylated subunits (GST·BITC and GST·2BITC; Table 3). In summary, upon treatment of GST P1-1 with an excess of BITC-SG, 1:1 and 1:2 covalent adducts were found after incubation for 3 h at 37 °C.

Table 3. ESI mass spectrometry and DTNB titration data of GST P1-1 and its mutant forms incubated with BITC–SG for 3 h at 37 °C (see Experimental Section for details).

Enzyme	**ESI mass spectrometry**		**DTNB titration**
	***M*$_W$ [Da]**	**Assignment**	**NCys[c]**
wild-type (wt)	23 225	[GST][a]	3.8
	23 356	[GST*][b]	
wt+BITC–SG	23 374	[GST][a]+BITC	1.1
	23 505	[GST*][b]+BITC	
	23 523	[GST][a]+2×BITC	

Enzyme	ESI mass spectrometry		DTNB titration
	M_W [Da]	Assignment	NCys[c]
	23 654	[GST*][b]+2×BITC	
C47S	23 208	[C47S]	2.1
C47S+BITC–SG	23 208	[C47S]	1.0
	23 357	[C47S]+BITC	
C47S/C101S	23 192	[C47S/C101S]	0.2
C47S/C101S+BITC–SG	23 191	[C47S/C101S]	0.2

[a] [GST]=[GST P1-1]. [b] [GST*]=[GST P1-1]+Met. [c] Number of cysteines (per dimer).

Similar mass experiments to those described above were performed with the C47S and C47S/C101S mutants. Ion spray mass spectra of the unmodified C47S (Figure 5 C) and C47S/C101S (Figure 5 E) mutants showed only one peak each with molecular masses of 23 208 and 23 192 Da, respectively. The molecular masses obtained for these mutants are in agreement with those deduced from the cDNA sequence after replacing cysteine with serine. Moreover, the presence of just one peak in the ESI mass spectra of these unmodified mutants indicates complete removal of the N-terminal methionine, as previously observed.12a The BITC–SG-incubated C47S mutant exhibits two major peaks, one at *m*/*z* 23 208 amu and another at *m*/*z* 23 357 amu, corresponding to the unmodified and modified subunits, respectively (Figure 5 D). The mass difference between these two major peaks is 149 Da, which matches well with the mass of the BITC moiety of BITC–SG. The peak areas for the modified and unmodified subunits are similar, indicating the incorporation of just one BITC group per enzyme dimer to form the BITC–S101 protein adduct with one of the Cys101 residues in the dimeric interface. Furthermore, the ESI spectrum of the BITC–SG-incubated C47S/C101S mutant exhibits the same peak at *m*/*z* 23 191 amu due to the unmodified subunit (Figure 5 F). Therefore, simultaneous replacement of the Cys47 and Cys101 residues by serine does not give rise to any adduct, corroborating that these two residues are the only ones involved in the covalent modification induced by the BITC–SG conjugate. In addition, the ESI spectrum of the

BITC–SG-incubated C101S mutant shows only a peak at *m*/*z* 23 357 amu, corresponding to the Cys47-modified subunit (see Supporting Information).

Moreover, direct titration of native GST P1-1 thiol groups (wild-type and C47S and C47S/C101S mutants) have been performed with thiol-specific reagent DTNB at 37 °C (see the Experimental Section for details). The results are shown in Table 3. Under the experimental conditions described herein, the ligand-free wild-type enzyme has four fast-reacting and DTNB-titrable thiol groups per dimer, as previously described.14 However, in the case of the ligand-free C47S and C47S/C101S mutants, only two or zero cysteine residues were titrable with DTNB per dimer, respectively (Table 3). Conversely, when the enzymes were previously incubated with BITC–SG for 3 h at 37 °C (see the Experimental Section for details), the number of free cysteine residues capable of reacting with DTNB dropped to one per dimer in the case of the wild-type enzyme and the C47S mutant, or none for the double C47S/C101S mutant (Table 3).

Discussion

The results described in this paper indicate that the BITC–SG and BC–SG conjugates act as moderate competitive inhibitors for hGST P1-1. The binding of BITC–SG or BC–SG to wt-enzyme is non-cooperative, with a 1:1 stoichiometry (one molecule of ligand per subunit; Figure 1 A) across temperature ranges of 8 to 23 °C or 19 °C to 42 °C, respectively. In both cases, the affinities and inhibitory potencies are high, although they are lower for BC–SG than for BITC–SG (Tables 1 and 2). These GS-conjugates bind to wt-GST at the G and H sites in each monomer, with the conjugate GS-moiety occupying the G site and the BITC moiety the H-site. The thermodynamic parameters for these binding interactions are only measurable at the temperature ranges indicated above, across which they were enthalpically favorable but entropically unfavorable (Table 1), in agreement with the results obtained for other GS-conjugates.18, 19, 26 This suggests that although the interaction between BC–SG and the wt-enzyme is enthalpically more favorable (albeit slightly) than for BITC–SG, the entropic loss due to binding is also increased, implying that the –NH–CO– group in BC–SG makes the binding more enthalpically favorable but also more entropically unfavorable than –NH–CS–S–. The extra unfavorable entropy change outweighs the slight enthalpic advantage, resulting in a lower binding affinity for BC–SG (Table 1).

The temperature dependency of the global ΔH and $-T\Delta S^0$ changes for the binding of both GS conjugates to wt-GST P1-1 exhibits an enthalpic–entropic compensation and, as a consequence, ΔG^0 remains relatively constant with temperature. In addition, a negative heat

capacity change was also obtained for both GS conjugates, although slightly more negative for BC–SG. Therefore, the observed global behavior for the binding of these GS conjugates to this enzyme across the indicated temperature range, is very similar to that which was described for the binding of other GS conjugates.18, 19

From the calorimetric thermograms for the interaction of BITC–SG to wt-GST P1-1 at temperatures above 25 °C, a slow kinetic process was detected, concomitant to the binding process. A plausible mechanism with at least two separate steps is postulated: firstly, a reversible binding of BITC–SG (fast exothermic phase, step 1), followed by an irreversible reaction (slow endothermic phase) originated by covalent modification of the enzyme (step 2). As titration of the enzymes with DTNB reveals that only cysteines are modified by the binding of BITC–SG (Table 3), we chose Cys47 and Cys101 as potential candidates for this covalent modification. Certain studies with GST P1-1 stated that Cys47 and Cys101 are the most reactive among the four cysteines in each subunit toward electrophilic compounds14, 20, 27 or transition-metal-based compounds.12c,12d, 28 Additional studies have also shown that Cys47 acts as a target of electrophilic reagents such as 7-fluoro-4-sulfamoil-2,1,3-benzoxadiazole,29 BITC,17 GSNO,22, 30 EA,19 and E-SG.31 Equivalent cysteine residues (Cys45 and Cys99) in porcine GST π were modified by monobromobimane.32 Our ITC, mass spectrometry, and DTNB titration experiments indicate that Cys47 and Cys101 are indeed the targets of the BITC moiety generated by the binding and subsequent breakdown of BITC–SG at physiological temperature.

The high reactivity of Cys47 might rely on the particular position of this residue. It is located at the end of the flexible α2 helix, in contact with the solvent and close to the G site (10.7 Å from the sulfur atom in GSH), with its thiol group pointing toward a small hydrophobic pocket formed by the main chain atoms of Gln 51 and Lys 44 and the side chain atoms of Trp 38 and Leu 52. It has a pK_a value of 4.2 in GST P1-1 and may exist as an ion pair with the protonated ε-amino group of Lys 54 under physiological conditions.33 Thus, the α2 helix mobility increases with temperature, making it more accessible to the solvent and capable of acting as the preferential target for S-thiocarbamoylation by BITC–SG. In addition, both Cys101 residues are placed in front of one another at the dimer interface (see molecular docking under Experimental Section). The reactivity of this cysteine residue has also been proven, though it is less reactive than Cys47, toward a large number of electrophilic reactants.12c,12d, 23 The lesser reactivity of Cys101 toward S-thiocarbamoylation, compared to that of Cys47, was also shown by ITC (Figure 4). The calorimetric trace acquires a two-humped form when the wild-

type enzyme is titrated with a large excess of BITC–SG at 39 °C. Titration of Cys47 and Cys101 generate the first and second peaks, respectively. As can be observed from our data, the kinetic rate for the reaction of Cys101 with the BITC–SG conjugate is slower (τ=12 min) than for Cys47 (τ=4 min). These results also demonstrate the different reactivity of both cysteines toward S-thiocarbamoylation, in agreement with what was described in the literature for other electrophilic reagents.12c,12d, 22

Therefore, two behaviors were observed within the temperature range used in this work (8–42 °C). The effects at high temperatures (e.g., around 37 °C) are likely to be the physiologically most relevant scenarios, whereas the BITC–SG molecule acts as an electrophilic agent toward GST P1-1 inside the cell. At temperatures below 25 °C, covalent binding and adduct formation with these cysteine residues was undetected. Thus, at low temperatures, the covalent reaction with the cysteine residues is too small and therefore negligible in comparison with the strong exothermic binding. Accordingly, the interaction of BITC–SG with the wild-type enzyme at temperatures below 25 °C shows the typical ITC profile for a non-covalent binding to two equal and independent sites.

In addition, mass spectrometry and DTNB titrations have demonstrated that the Cys47 residues in both subunits are targets against BITC–SG, whereas only one Cys101 per dimer is covalently modified to form a BITC–Cys101 adduct. In order to find an explanation for this fact, it is necessary to take into account that the covalent attachment of a group of BITC on a Cys101 residue implies the previous binding of one molecule of the BITC–SG conjugate in a suitable mode and close to the Cys101 nucleophile (Scheme 1). Thus, if one of the two Cys101 remains unmodified, it might be due to the lack of noncovalent binding between the protein and a second molecule of BITC–SG. Most likely, the presence of the first BITC moiety covalently bound to one of the Cys101 residues hinders the accommodation of a second BITC–SG ligand molecule in the dimer interface. Our docking studies appear to support this hypothesis. Both Cys101 residues are located at the dimer interface, with their sulfur atoms pointing toward one another in a stalactite/stalagmite fashion, at a distance of 5.9 Å. Figure 6 depicts one of the best docking poses for BITC–SG in the dimer interface, according to the criterion explained in the Experimental Section. As the relative rmsd values for all of the chosen poses is less than 1.06 Å, the pose shown is very representative. All of the poses accommodate the two oxygens of the ligand GS moiety glutamyl carboxylic acid at a distance of 2.2 Å each from the terminal NH_2 of Asn 110, inside a hydrophilic pocket formed by Ser 105, Leu 106, and Asn 110, the surface of which is color-coded in the figure, whilst the ligand BITC moiety aromatic ring is

oriented perpendicular to the middle □CH_3 on the side chain of Ile 104 at a distance of 3.5 Å. The yellow surface patches correspond to both Cys101 sulfur atoms, whilst the thick light gray structure bound to one of them depicts a covalently bound BITC moiety. It is clear from this figure than the second BITC–SG molecule would overlap the previous covalently bound BITC if it was to bind. Thus, the BITC moiety that first attaches to one Cys101 protects the other against covalent inactivation by a second molecule of BITC.

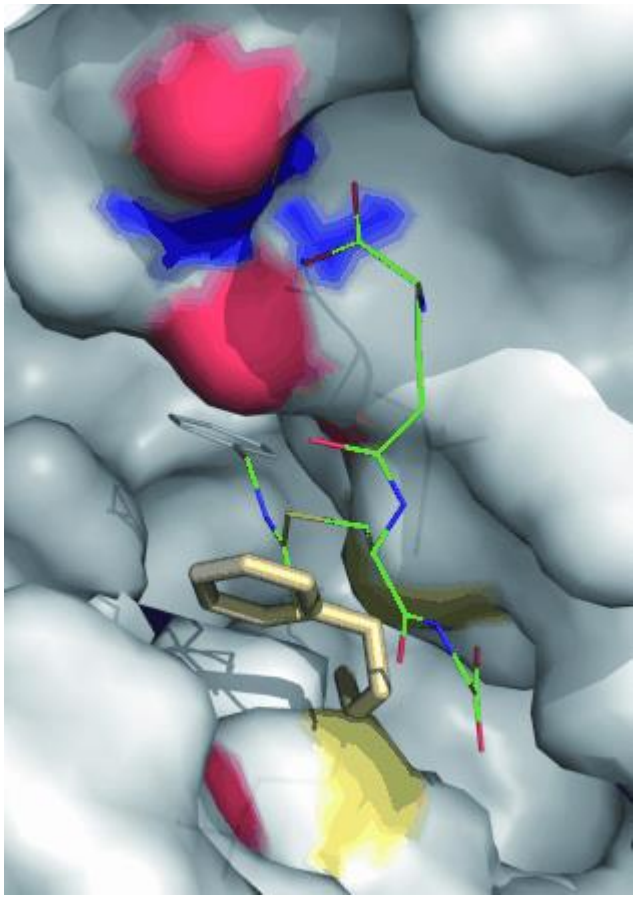

Figure 6 Depiction of the GST P1-1 dimer interface at the Cys101 site. The large gray patch corresponds to the enzyme surface. The two Cys101 residues are depicted as a yellow patch in both subunits, and their side-chain stick representations can be seen through the transparent enzyme surface. A BITC moiety, depicted as a thick brown stick representation, is covalently attached to the sulfur atom of one of the cysteines. The thin atom-color-coded ligand represents a docked BITC–SG conjugate molecule bound to the enzyme in a mode suitable to be attacked by a Cys101 residue, whilst the red and blue surfaces of the enzyme represent the residues forming a hydrophilic pocket wrapped around the ligand GS moiety glutamyl carboxylic acid, locking it into position. It is evident from this figure that the presence of a covalently attached BITC moiety hinders the binding of a second BITC–SG molecule.

It is worth mentioning that, in this study, BITC covalent modification occurring on cysteine residues 47 and 101 takes place in the presence of a large excess of BITC–SG and the initial absence of GSH. Under these conditions, the reversibility of the transthiocarbamoylation reaction6 is most likely negligible. However, when a cysteine residue is modified by BITC–SG through the covalent attachment of its BITC moiety, an equimolar quantity of free GSH is released. Thus, BITC binds to the enzyme in a productive mode, different from the nonproductive mode that occurs in the total absence of GSH. Similar behavior was observed for the binding of EA to GST P1-1.34 Moreover, the binding of EA also generated two covalent adducts with Cys47 and Cys101.21 Therefore, we propose that the observed covalent binding of BITC reported herein occurs in a similar fashion. Finally, when our results are compared to those obtained previously for the binding of BITC to GST P1-1,17 the different modification sites in the enzyme can be explained as a consequence of the different reactivities of BITC and the S-thiocarbamate. Thus, both results indicate the capability of GST P1-1 to discriminate between a GS–xenobiotic conjugate and its parent xenobiotic. We believe that this important fact should be taken into account when designing inhibitors.

Experimental Section

Materials: GSH, 1-chloro-2, 4-dinitrobenzene (CDNB), BITC, 5,5'-dithiobis-(2-nitrobenzoic acid) (DTNB), and EA were purchased from Sigma. EASG was synthesized as described previously.19 The construction, purification, and characterization of wild-type GST P1-1 enzyme and the three mutants (C47S, C101S, and C47S/C101S) were described previously.20, 21, 25 Other chemicals employed were of the highest available purity.

General methods: TLC was performed on Merck Silica Gel 60 F254 aluminium sheets and developed by UV light and phosphomolybdic acid (8 % in EtOH). Flash column chromatography was performed on Merck Silica Gel (230–400 mesh, ASTM). ^{1}H and ^{13}C NMR spectra were recorded on Bruker Avance DPX 300 MHz and Varian VNMRS 500 MHz spectrometers. Chemical shifts are given in ppm and referenced to internal TMS (δ_H, δ_C=0.00 ppm). *J* values are given in Hz. COSY, HMQC and HMBC experiments were used when necessary for unequivocal assignment. Optical rotations were recorded on a Jasco P-1030 polarimeter at room temperature. $[\alpha]_D$ values are given in 10^{-1} deg cm^2 g^{-1}. Melting points were measured on a Büchi B-450 melting point apparatus and are uncorrected. IR spectra were measured on a PerkinElmer Spectrum One FT-IR spectrometer equipped with a PerkinElmer universal ATR sampling accessory. Electrospray (ESI) mass spectra were performed in the presence of formic acid (0.1 %) on a Waters XEVO QTof spectrometer.

Synthesis of BITC–SG and BC–SG conjugates: Each conjugate was prepared by applying a different methodology (see the Supporting Information for details). Conjugation of GSH with benzyl isothiocyanate (BITC) was accomplished by modifying a published method.17 Glutathione was combined with BITC in H_2O/MeCN (1:3) for 3 days at room temperature. An excess of BITC was used to ensure complete consumption of GSH and hence simplify the purification step. BITC–SG conjugate was obtained in 62 % yield after washing with acetone to remove all unreacted BITC and enable recrystallization from water. Separately, the disodium salt of *S*-(*N*-benzylcarbamoylmethyl)glutathione (BC–SG) was prepared by mixing GSH with an excess of *N*-benzyl-2-chloroacetamide in H_2O/EtOH (1:1) in the presence of $NaHCO_3$. Once the reaction was complete, the solvent was removed by evaporation under vacuum, and the crude compound was purified by column chromatography and lyophilized. BITC–SG and BC–SG conjugates were characterized by NMR and electrospray mass spectrometry. Results were consistent with the expected structures and showed no traces of free GSH. ^{1}H NMR data for BITC–SG in [D_6]DMSO agreed with those previously published.35 The stability of BITC–SG was tested by NMR in D_2O at 1 mM. Under these conditions, this compound is stable in solution for at least 24 h.

Inhibition of GST P1-1 activity by BITC–SG and BC–SG: Varying concentrations of BITC–SG and BC–SG (0.1–200 μM), pre-dissolved in potassium phosphate buffer (0.1 M, pH 7.0), were added to a reaction mixture of potassium phosphate buffer (1 mL (final volume), 0.1 M, pH 6.5), containing GSH (1 mM) and about GST P1-1 (1 μg). The residual activity of GST P1-1 was assayed spectrophotometrically at 340 nm (ε=9600 M^{-1} cm^{-1}) upon addition of the substrate 1-chloro-2,4-dinitrobenzene (CDNB, final concentration 1 mM), at 25 °C. The IC_{50} value for the inhibition of GST activity was determined by fitting the plot of residual GST activity against the inhibitor concentration with a sigmoidal dose–response function using Graph PAD Prism 4.0 (Graph PAD Software, San Diego, CA). The apparent K_m and V_{max} values of GST P1-1 were also determined in the presence of BITC–SG and BC–SG. Kinetic data were collected by varying GSH (0.02–1 mM) at a fixed CDNB concentration (1 mM), with fixed concentrations of inhibitors (20, 50, 100, 200 μM). Apparent K_m and V_{max} values were obtained from Lineweaver–Burk plots using Graph PAD Prism. K_i(GSH) values were derived from the different sets of reciprocal plots.

Fluorescence spectroscopy: Intrinsic fluorescence of GST P1-1 was measured with a PTI QuantaMaster (QM4-CW) spectrofluorometer equipped with a Peltier device and associated with a Biologic SFM/20 titration accessory. The experimental conditions and data analysis were similar to those described elsewhere.19, 22 Briefly, a number of samples containing 2–4 μM of

GST in sodium phosphate buffer (2 mL, 20 mM, containing 5 mM NaCl and 0.1 mM EDTA) at pH 7.0 were added to a 3 mL quartz fluorescence cell, and the fluorescence intensity was measured. A suitable amount of the conjugate dissolved in the same buffer was then added to each sample, and the fluorescence intensity was measured after mixing. Measurements were corrected for dilution and inner filter effects.

Electrospray mass spectrometry: In order to determine whether GSTs are covalently modified by BITC–SG, we incubated the proteins (10 μM) with BITC–SG (500 μM) in 10 mM sodium phosphate, pH 7.0, at 37 °C for 3 h. The samples were then dialyzed exhaustively against the same buffer to remove any excess reagent and were lyophilized for mass spectrometry studies. Samples of control proteins were treated in the same manner but without additional BITC–SG. Proteins were reconstituted by solubilizing the lyophilized powder in H_2O (50 μL). Each sample (2 μL; 1:20, *v*/*v*) was injected into an HPLC Agilent 1100 system. The mobile phase was composed of ACN/H_2O (50:50) and +0.1 % formic acid, delivered at 100 μL min^{-1}. Spectra were obtained in positive mode using a capillary voltage of +4 kV, with a source temperature of 300 °C and fragment voltage of +300 V. Spectra were scanned over *m*/*z* 500–2500 at 20 s per scan and summed. Mathematical transformations of electrospray spectra to true mass scale were obtained by the MaxEnt algorithm (Fisons Masslynx software). It is interesting to note that the presence of sodium ions in the buffer solution resulted in additional peaks of decreased intensity emerging after the main peaks, due to sodium addition during the ionization process in the positive ion detection mode.

Spectrophotometric determination of thiol groups: To evaluate the number of thiol groups in the enzymes noncovalently modified by BITC–SG, we titrated them following the Ellman's procedure.36 Control experiments with the native intact protein were also performed. Firstly, in order to regenerate completely the thiol residues in the enzymes, the protein samples were placed in phosphate buffer with β-mercaptoethanol as a reducing agent (50 mM sodium phosphate, 0.1 M β-mercaptoethanol, pH 7.0 at 25 °C) for 10 min. To remove the reducing agent, the protein samples were passed through a Sephadex G-25 column equilibrated in 50 mM sodium phosphate, pH 7.0. The eluted samples (about 100 μg of wild-type or C47S, C101S, or C47S/C101S mutant enzymes) were pooled and incubated for 3 h at 37 °C in the presence of 500 μM BITC–SG. Next, in order to remove any excess of this reactant, the samples were passed again through the Sephadex G-25 column equilibrated in 50 mM sodium phosphate, pH 7.0. The eluted samples were reacted with DTNB (15 mM) in phosphate buffer (1 mL (final volume), 50 mM, pH 7.0), at 20 °C for 30 min. Finally, the absorbance of the samples was

measured spectrophotometrically at 412 nm.36 The same procedure, but without BITC–SG treatment, was applied to control protein aliquots and used as a reference for comparison purposes.

Isothermal titration calorimetry (ITC): Calorimetric experiments were conducted in an ultrasensitivity VP-ITC instrument (MicroCal Inc., Northampton, MA). Sample preparation and ITC experiments were carried out as previously described elsewhere.19, 23, 37 Titrations were routinely performed in sodium phosphate (20 mM), NaCl (5 mM), and EDTA (0.1 mM) at pH 7.0. Phosphate buffer was chosen by virtue of its small ionization enthalpy change; hence, the measured binding enthalpies have a negligible contribution due to buffer protonation. Blank titrations of ligand into buffer alone were also performed to correct for heat generated by dilution and mixing. Two models have been used to fit the experimental data: an equal and independent sites model (non-cooperative model) and a two equal and interacting sites model (cooperative model). The experimental data were fitted using Scientist software (Micromath Scientific Software, St. Louis, MO, USA) to the model algorithms implemented by us. The equations used in these models have been widely described in literature.37, 38 Finally, changes in standard free energy ΔG^0 and entropy ΔS^0 were determined as $\Delta G^0 = -RT \ln K$ and $T\Delta S^0 = \Delta H - \Delta G^0$ (assuming that $\Delta H = \Delta H^0$).

Molecular docking: BITC–SG and BC–SG were constructed by gluing together their moieties with the help of Avogadro 1.01,39 taking special care to keep the bond distances and angles at the correct values, as follows: 1) BITC and BC structures were built by importing their name structures and applying a geometry optimization afterward; 2) the BITC and BC moieties were glued to the G site bound GS moiety from PDB ID: 11GS. This PDB structure contains the ethacrynic acid-glutathione conjugate bound to GST P1-1, which is the most similar conjugate to the ones we are studying among the known GST P1-1 X-ray structures. We chose to proceed in this manner because we believe that a moiety based on a crystallographic measurement is more reliable than a computer generated guess. The GST P1-1 protein structure used for docking was also taken from the 11GS PDB entry following removal of the ligand and water molecules, to ensure the closest possible enzyme structure.

AutoDockTools 1.5.440 was used to prepare the protein and the ligands prior to the docking studies. Atomic Gasteiger partial charges and polar hydrogens were added. The protein structure was considered as a rigid body, as was the G-site-binding GS moieties of the ligands. The rest of the ligand structures were kept flexible with automatic detection of the active rotatable bonds. The reason for maintaining the unrotatable nature of the G-site-binding GS

moiety in the constructed ligands is based on the fact that its binding mode does not change regardless of the conjugate bound to GST. This is easily seen when superimposing all of the corresponding published GST P1-1 X-Ray structures (more than 20 to date). Thus, we chose to preserve this structure and leave it untouched by the docking process.

To model the GST P1-1 interaction with BITC–SG at the G and H binding sites, docking experiments were performed with AutoDock Vina 1.1.1,41 which is based on the Iterated Local Search global optimiser algorithm.42 The runs were performed with an exhaustiveness of 256 and the search space within the subunit A active site at an *x*,*y*,*z* position of 10,5.5,26 and widths of 14, 12 and 11 Å for the *x*-, *y*- and *z*-axes, respectively. This box covers the whole G and H site space required by the ligand. In order to select the best BITC–SG binding conformations among the candidates proposed by Vina, we were guided by the binding mode of the ligand GS moiety in the G site. We saved as hits poses that exactly mimicked the binding modes of the published crystallographic structures.

To model the GST P1-1 interaction with BC–SG, we followed exactly the same procedure as for BITC–SG, with an identical box as the search space. A close examination of the dimer interface reveals that both Cys101 residues in the GST P1-1 structure are placed in front of one another at the dimer interface, with their reduced sulfurs only 5.9 Å away, resembling a stalactite/stalagmite formation. Therefore, to model the GST P1-1 interactions with BITC–SG and BITC, we chose a box centered on the line connecting both Cys101 sulfur atoms as the search space. The box used for BITC had *x*, *y*, and *z* widths of 10 Å each, whilst for the glutathione conjugate we used a larger box, with *x*, *y*, and *z* widths of 24, 14, and 20 Å, respectively. To select the most probable binding modes for both compounds among the proposed poses by the docking program, we chose the modes for which the reactive dithiocarbamoyl C□S carbon in the ligands was as close as possible to either of the Cys101 sulfur atoms, as we show from our mass spectrometry data that a covalent bond is formed between them. The best hits for BITC according to the above criterion show the dithiocarbamoyl C□S carbon at distances of 3.5 and 3.8 Å, respectively, to both Cys101 sulfurs, with its aromatic ring in close planar contact with one of the Cys101 protein surfaces. In the case of the BITC–SG conjugate, the dithiocarbamoyl C□S carbon in the chosen hits are at distances from both sulfur atoms of 4.4 and 5.8 Å, respectively. The driving force for this binding mode to lock into position seems to be the accommodation of the ligand GS moiety glutamyl carboxylic acid in a hydrophilic pocket formed by Ser105, Leu106, and Asn110, with

the BITC moiety aromatic ring oriented perpendicularly to the middle □CH_3 in the side chain of Ile104. All of the selected binding modes superimpose very well at these spots.

Acknowledgements

The authors acknowledge financial support from the Spanish Ministry of Science and Innovation and the EU European Regional Development Fund (Grant CTQ2010–17848), as well as the Andalusian Government (Consejería de Economía, Innovación y Ciencia, Junta de Andalucía, grants CVI-6028 and FQM-3141).

- 1 a) Y. Zhang, P. Talalay, *Cancer Res.* 1994, **54**, 1976–1981; b) Y. Zhang, S. Yao, J. Li, *Proc. Nutr. Soc.* 2006, **65**, 68–75; c) Y. Zhang, *Mol. Nutr. Food Res.* 2010, **54**, 127–135; d) S. S. Hecht, *Drug Metab. Rev.* 2000, **32**, 395–411; e)C. C. Conaway, Y. M. Yang, F. L. Chung, *Curr. Drug Metab.* 2002, **3**, 233–255.
- 2 a) S. S. Hecht, *J. Cell. Biochem.* 1995, 22 (Suppl.), 195–209; b) P. Talalay, *Adv. Enzyme Regul.* 1989, **28**, 237–250; c) Z. Guo, T. J. Smith, E. Wang, K. Eklind, F.-L. Chung, C. S. Yang, *Carcinogenesis* 1993, **14**, 1167–1173; d) M. A. Morse, G. D. Stoner, *Carcinogenesis* 1993, **14**, 1737–1746; e) Y. Zhang, P. Talalay, *Cancer Res.* 1998, **58**, 4632–4639.
- 3 L. Mi, Z. Xiao, T. D. Veenstra, F.-L. Chung, *J. Proteomics* 2011, **74**, 1036–1044.
- 4 a) R. H. Klom, U. H. Danielson, Y. Zhang, P. Talalay, B. Mannervik, *Biochem. J.* 1995, **311**, 453–459; b) D. J. Meyer, D. J. Crease, B. Ketterer, *Biochem. J.* 1995, **306**, 565–569; c) Y. Zhang, R. H. Kolm, B. Mannervik, P. Talalay, *Biochem. Biophys. Res. Commun.* 1995, **206**, 748–755.
- 5 D. Podhradský, L. Drobnica, P. Kristian, *Experientia* 1979, **35**, 154–155.
- 6 T. Shibata, Y. Kimura, A. Mukai, H. Mori, S. Ito, Y. Asaka, S. Oe, H. Tanaka, T. Takahashi, K. Uchida, *J. Biol. Chem.* 2011, **286**, 42150–42161.
- 7 a) B. Mannervik, U. H. Danielson, *CRC Crit. Rev. Biochem.* 1988, **23**, 283–337; b) B. Mannervik, P. G. Board, J. D. Hayes, I. Listowsky, W. R. Pearson, *Methods Enzymol.* 2005, **401**, 1–8.
- 8 a) A. Aceto, C. Di Ilio, S. Angelucci, M. Felaco, G. Federici, *Biochem. Pharmacol.* 1989, **38**, 3653–3660; b) C. S. Morrow, P. K. Smitherman, S. K. Diah, S. Erasmus, A. J. Townsend, *J. Biol. Chem.* 1998, **273**, 20114–20120; c) D. M.

Townsend, V. L. Findlay, K. D. Tew, *Methods Enzymol.* 2005, **401**, 287–307; d) D. M. Townsend, K. D. Tew, *Oncogene* 2003, **22**, 7369–7375.

- 9 a) L. Gaté, K. D. Tew, *Expert Opin. Ther. Targets* 2001, **5**, 477–489; b) G. Zhao, X. Wang, *Curr. Med. Chem.* 2006, **13**, 1461–1471; c) P. Ruzza, A. Rosato, C. R. Rossi, M. Floreani, L. Quintieri, *Anti-cancer Agents Med. Chem.* 2009, **9**, 763–777.
- 10 a) S. Mahajan, W. M. Atkins, *Cell. Mol. Life Sci.* 2005, **62**, 1221–1233; b) G. A. Morales, E. Laborde, *Annu. Rep. Med. Chem.* 2007, **42**, 321–335.
- 11 D. J. Meyer, *Xenobiotica* 1993, **23**, 823–834.
- 12 a) A. E. Mitchell, J. Zheng, B. D. Hammock, M. Lo Bello, A. D. Jones, *Biochemistry* 1998, **37**, 6752–6759; b) G. Ricci, F. De Maria, G. Antonini, P. Turella, A. Bullo, L. Stella, G. Filomeni, G. Federici, A. M. Caccuri, *J. Biol. Chem.* 2005, **280**, 26397–26405; c) W. H. Ang, A. De Luca, C. Chapuis-Bernasconi, L. Juillerat-Jeanneret, M. Lo Bello, P. J. Dyson, *ChemMedChem* 2007, **2**, 1799–1806; d) W. H. Ang, L. J. Parker, A. De Luca, L. Juillerat-Jeanneret, C. J. Morton, M. Lo Bello, M. W. Parker, P. J. Dyson, *Angew. Chem.* 2009, **121**, 3912–3915; *Angew. Chem. Int. Ed.* 2009, **48**, 3854–3857; e) B. Van Ommen, J. M. Ploemen, J. J. Boggards, T. J. Monks, S. S. Gau, P. J. Van Bladeren, *Biochem. J.* 1991, **276**, 661–666; f) J. Wang, S. Bauman, R. F. Colman, *J. Biol. Chem.* 2000, **275**, 5493–5503.
- 13 R. R. Rando, *Pharmacol. Rev.* 1984, **36**, 111–142.
- 14 G. Ricci, G. Del Boccio, A. Pennelli, M. Lo Bello, R. Petruzzelli, A. M. Caccuri, D. Barra, G. Federici, *J. Biol. Chem.* 1991, **266**, 21409–21415.
- 15 M. Lo Bello, R. Petruzzelli, E. De Stefano, C. Tenedini, D. Barra, G. Federici, *FEBS Lett.* 1990, **263**, 389–391.
- 16 a) K. Tamai, H. X. Shen, S. Tsuchida, I. Hatayama, K. Satoh, A. Yasui, A. Oikawa, K. Sato, *Biochem. Biophys. Res. Commun.* 1991, **179**, 790–797; b) A. M. Caccuri, R. Petruzzelli, F. Polizio, G. Federici, A. Desideri, *Arch. Biochem. Biophys.* 1992, **297**, 119–122; c) M. L. Van Iersel, J. P. Ploemen, M. Lo Bello, G. Federici, P. J. van Bladeren, *Chem.-Biol. Interact.* 1997, **108**, 67–78.
- 17 L. A. Ralat, R. F. Colman, *J. Biol. Chem.* 2004, **279**, 50204–50213.
- 18 E. Ortiz-Salmerón, M. Nuccetelli, A. J. Oakley, M. W. Parker, M. Lo Bello, L. García-Fuentes, *J. Biol. Chem.* 2003, **278**, 46938–46948.

- 19 I. Quesada-Soriano, L. J. Parker, A. Primavera, J. M. Casas-Solvas, A. Vargas-Berenguel, C. Barón, C. J. Morton, A. P. Mazzetti, M. Lo Bello, M. W. Parker, L. García-Fuentes, *Protein Sci.* 2009, **18**, 2454–2470.
- 20 M. Lo Bello, A. Battistoni, A. P. Mazzetti, P. G. Board, M. Muramatsu, G. Federici, G. Ricci, *J. Biol. Chem.* 1995, **270**, 1249–1253.
- 21 G. Ricci, M. Lo Bello, A. M. Caccuri, A. Pastore, M. Nuccetelli, M. W. Parker, G. Federici, *J. Biol. Chem.* 1995, **270**, 1243–1248.
- 22 R. Téllez-Sanz, E. Cesareo, M. Nuccetelli, A. M. Aguilera, C. Barón, L. J. Parker, J. J. Adams, C. J. Morton, M. Lo Bello, M. W. Parker, L. García-Fuentes, *Protein Sci.* 2006, **15**, 1093–1105.
- 23 I. Quesada-Soriano, L. J. Parker, A. Primavera, J. Wielens, J. K. Holien, J. M. Casas-Solvas, A. Vargas-Berenguel, A. M. Aguilera, M. Nuccetelli, A. P. Mazzetti, M. Lo Bello, M. W. Parker, L. García-Fuentes, *J. Mol. Recognit.* 2011, **24**, 220–234.
- 24 P. E. Morin, E. Freire, *Biochemistry* 1991, **30**, 8494–8500.
- 25 A. Battistoni, A. P. Mazzetti, R. Petruzzelli, M. Muramatsu, G. Federici, G. Ricci, M. Lo Bello, *Protein Expression Purif.* 1995, **6**, 579–587.
- 26 E. Ortiz-Salmerón, Z. Yassin, M. J. Clemente-Jimenez, F. J. Las Heras-Vazquez, F. Rodriguez-Vico, C. Barón, L. García-Fuentes, *Biochim. Biophys. Acta Protein Struct. Mol. Enzymol.* 2001, **1548**, 106–113.
- 27 H. J. Park, K. S. Lee, S. H. Cho, K. H. Kong, *Bull. Korean Chem. Soc.* 2001, **22**, 77–83.
- 28 E. Cesareo, L. J. Parker, J. Z. Pedersen, M. Nuccetelli, A. P. Mazzetti, A. Pastore, G. Federici, A. M. Caccuri, G. Ricci, J. J. Adams, M. W. Parker, M. Lo Bello, *J. Biol. Chem.* 2005, **280**, 42172–42180.
- 29 J. Nishihira, T. Ishibashi, M. Sakai, N. Shinzo, T. Kumazaki, Y. Hatanaka, S. Tsuda, K. Hikichi, *Biochem. Biophys. Res. Commun.* 1992, **188**, 424–432.
- 30 M. Lo Bello, M. Nuccetelli, A. M. Caccuri, L. Stella, M. W. Parker, J. Rossjohn, W. J. McKinstry, A. F. Mozzi, G. Federici, F. Polizio, J. Z. Pedersen, G. Ricci, *J. Biol. Chem.* 2001, **276**, 42138–42145.
- 31 C. Ibarra, M. P. Grillo, M. Lo Bello, M. Nucettelli, T. K. Bammler, W. M. Atkins, *Arch. Biochem. Biophys.* 2003, **414**, 303–311.
- 32 L. A. Ralat, R. F. Colman, *Protein Sci.* 2003, **12**, 2575–2587.

- 33 M. Lo Bello, M. W. Parker, A. Desideri, F. Polticelli, M. Falconi, G. Del Boccio, A. Pennelli, G. Federici, G. Ricci, *J. Biol. Chem.* 1993, **268**, 19033–19038.
- 34 a)A. J. Oakley, J. Rossjohn, M. Lo Bello, A. M. Caccuri, G. Federici, M. W. Parker, *Biochemistry* 1997, **36**, 576–585; b) A. J. Oakley, M. Lo Bello, A. P. Mazzetti, G. Federici, M. W. Parker, *FEBS Lett.* 1997, **419**, 32–36.
- 35 G. Brüsewitz, B. D. Cameron, L. F. Chasseaud, K. Görler, D. R. Hawkins, H. Koch, W. H. Mennicke, *Biochem. J.* 1977, **162**, 99–107.
- 36 G. L. Ellman, *Arch. Biochem. Biophys.* 1959, **82**, 70–77.
- 37 L. García-Fuentes, R. Téllez-Sanz, I. Quesada-Soriano, C. Barón in *Thermodynamics: Physical Chemistry of Aqueous Systems* (Ed.:), InTech, Rijeka, 2011, pp. 1–26.
- 38 J. Wyman, S. J. Gill in *Binding and linkage: Functional chemistry of biological macromolecules*, University Science Books, Mill Valley, 1990, pp. 123–163.
- 39 *Avogadro: An Open-Source Molecular Builder and Visualization Tool*, *Version 1.01*, http://avogadro.openmolecules.net/.
- 40 M. F. Sanner, *J. Mol. Graphics Modell.* 1999, **17**, 57–61.
- 41 O. Trott, A. J. Olson, *J. Comput. Chem.* 2010, **31**, 455–461.
- 42 a) J. Baxter, *J. Oper. Res. Soc.* 1981, **32**, 815–819; b) *Hybrid Metaheuristics: An Emerging Approach to Optimization* (Eds.:), Springer-Verlag, Berlin, 2008.